ACADEMIC PRESS

Available online at www.sciencedirect.com

SCIENCE DIRECT®

Journal of Sound and Vibration 260 (2003) 693–709

JOURNAL OF SOUND AND VIBRATION

www.elsevier.com/locate/jsvi

Vibration of tapered Mindlin plates in terms of static Timoshenko beam functions

Y.K. Cheung[a], D. Zhou[b,*]

[a] *Department of Civil Engineering, The University of Hong Kong, Hong Kong*

[b] *Department of Applied Mechanics and Civil Engineering, Nanjing University of Science and Technology, Nanjing 210014, People's Republic of China*

Received 17 August 2001; accepted 7 May 2002

Abstract

In this paper, the free vibrations of rectangular Mindlin plates with variable thickness in one or two directions are investigated. The thickness variation of the plate is continuous and can be represented by a power function of the rectangular co-ordinates. A wide range of tapered rectangular plates can be described by giving various index values to the power function. Two sets of new admissible functions are developed, respectively, to approximate the flexural displacement and the angle of rotation due to bending of the plate. The eigenfrequency equation is obtained by using the Rayleigh–Ritz method. The complete solutions of displacement and angle of rotation due to bending for a tapered Timoshenko beam (a strip taken from the tapered Mindlin plate in some direction) under a Taylor series of static load have been derived, which are used as the admissible functions of the rectangular Mindlin plates with taper thickness in one or two directions. Unlike conventional admissible functions which are independent of the thickness variation of the plate, the static Timoshenko beam functions presented in this paper are closely connected with the thickness variation of the plate so that higher accuracy and more rapid convergence can be expected. Some numerical results are furnished for both truncated Mindlin plates and sharp-ended Mindlin plates. On the basis of convergence study and comparison with available results in literature, it is shown that the first few eigenfrequencies can be obtained with quite satisfactory accuracy by using only a small number of terms of the static Timoshenko beam functions.

*Corresponding author. Tel.: +852-2859-2666; fax: +852-2559-5337.

E-mail address: hreccyk@hkucc.hku.hk (D. Zhou).

0022-460X/03/$ - see front matter
PII: S0022-460X(02)01008-8

1. Introduction

Vibration analysis of rectangular plates is necessary for designers to understand the dynamic behavior of many common structures. It is well known that the classical plate theory [1] has been successfully applied to the analysis of thin plates by assuming straight lines originally normal to the median-surface of plate remaining straight and normal after deformation. This classical plate theory, however, over-predicts the eigenfrequencies of higher modes for thin plates and even all the eigenfrequencies for thick plates where the effects of transverse shear deformation and rotary inertia become significant. Consequently, for enhancing the accuracy of analysis different kinds of refined plate theories were developed, in which the Mindlin plate theory [2,3] (relaxing the normality assumption and considering the effect of rotary inertia) has been widely employed in the analysis of moderately thick plates.

The analysis for vibration of rectangular thick plates with uniform thickness [4–9] and rectangular thin plates with variable thickness [10–12] has been extensively investigated by many investigators using various kinds of analytical and numerical methods. However, the analysis for vibration of rectangular thick plates with non-uniform thickness has received rather less attention and only very limited references can be found. Mikami and Yoshimura [13] are the first to study the vibration of rectangular Mindlin plates with non-uniform thickness, to the best of the authors' knowledge. They used the collocation method to analyze the free vibration of rectangular Mindlin plates with linearly varying thickness. The same problem was studied by Aksu and Al-Kaabi [14] using the variational principles in conjunction with the finite difference technique and by Mizusawa [15] using the spline strip method. In addition, Al-Kaabi and Aksu [16,17] extended their method to investigate the free vibration of rectangular Mindlin plates with bilinearly varying thickness and parabolically varying thickness, respectively. In all these studies, only plates with two opposite edges simply supported and varying thickness along one direction are examined. Moreover, Matsuda and Sakiyama [18] used a discrete method in conjunction with the integral equation technique to analyze the free vibration of skew Mindlin plates with variable thickness in one direction. A literature survey on the vibration analysis of thick plates can also be found [19].

In the present paper, two sets of admissible functions, describing the displacement and angle of rotation due to bending of the tapered Mindlin plate are developed from the complete solutions of the tapered Timoshenko beam under a Taylor series of static loads [20]. This tapered beam is considered to be a unit width strip taken from the tapered rectangular plate in the longitudinal direction or the vertical direction. Only the static Timoshenko beam functions in one direction needed to be derived because the tapered plates considered in this paper are with a similar pattern of thickness variation in both directions. As a result, the effects of both the shear correction factor and the thickness variation of the plate on the admissible functions have been considered so that more rapid convergence and higher accuracy can be achieved by using the static Timoshenko beam functions instead of using the conventional admissible functions.

2. The eigenfrequency equation of tapered plates

A tapered rectangular Mindlin plate with continuously varying thickness in both directions, as shown in Fig. 1(a), lies in the $x-y$ plane and is bounded by edges $x = \alpha A, A$ and $y = \beta B, B$ where

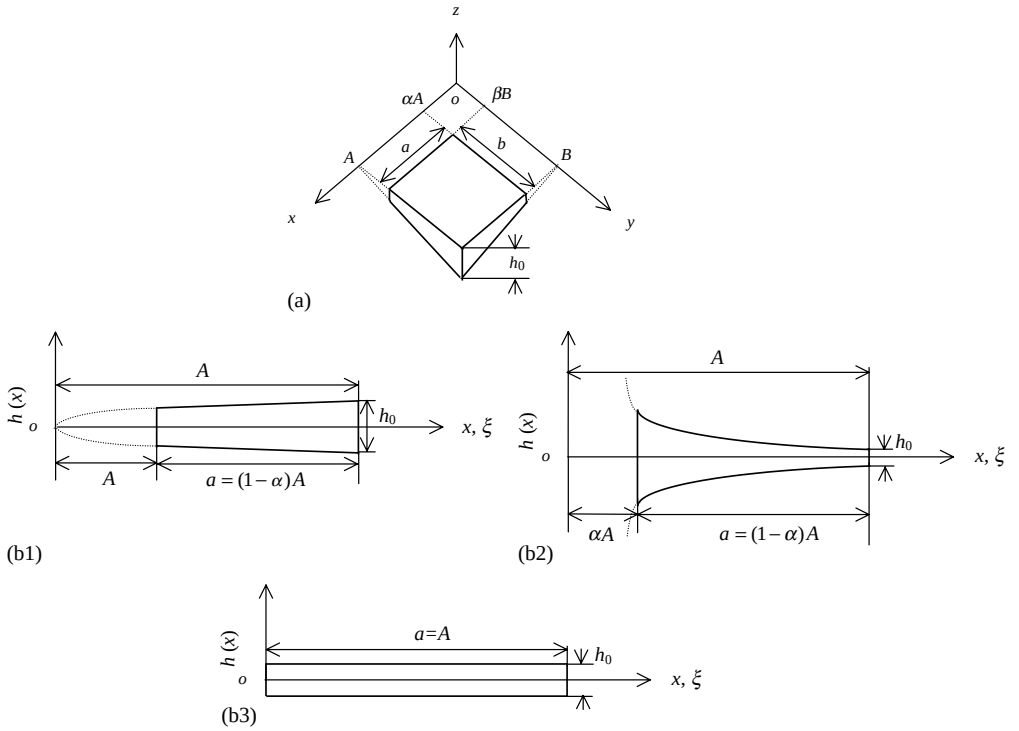

Fig. 1. Rectangular plate with variable thickness in two directions and a unit width strip taken from the plate in the x direction: (a) tapered rectangular plate, (b1) tapered beam for $r > 0$, (b2) tapered beam for $r < 0$ and (b3) uniform beam ($r = 0$).

$\alpha\,(0 \leqslant \alpha < 1)$ and $\beta\,(0 \leqslant \beta < 1)$ are referred to as truncation factors of the plate in the x and y directions, respectively. The side lengths of the plate are a and b in the x and y directions, respectively, where $a = (1 - \alpha)A$ and $b = (1 - \beta)B$. If the plate is with a sharp edge in the x direction then $\alpha = 0$ and if the plate is with a sharp end in the y direction then $\beta = 0$. Assuming that the thickness $h(x, y)$ can be written in a form of the power function as follows:

$$h(x, y) = h_0(x/A)^r(y/B)^s, \tag{1}$$

where h_0 is the thickness of the plate at $x = A, y = B$, r and s are referred to as taper factors of the plate in the x and y directions, respectively. A wide range of tapered rectangular plates can be described by giving various values to r and s. Some common tapered rectangular plates are shown in Table 1.

The energy functional Π for a rectangular Mindlin plate can be written in terms of the maximum strain energy U_{max} and the maximum kinetic energy T_{max} [7] as follows:

$$\Pi = U_{max} - T_{max}. \tag{2}$$

Table 1
Some common tapered rectangular plates

Type of the tapered rectangular plates	Taper factors
A uniform plate	$r=0$, $s=0$
A linearly tapered plate in the x direction	$r=1$, $s=0$
A linearly tapered plate in both directions	$r=1$, $s=1$
A parabolically tapered plate in the x direction	$r=2$, $s=0$
A parabolically tapered plate in both direction	$r=2,: s=2$
A hyperbolically tapered plate in the x direction	$r=-1$, $s=0$
A hyperbolically tapered plate in both directions	$r=-1$, $s=-1$

Table 1
Some common tapered rectangular plates

Introducing the non-dimensional co-ordinate $\xi = x/A$ and $\eta = y/B$, U_{max} and T_{max} are given, respectively, by

$$U_{max} = \frac{1}{2}\frac{D_0 B}{A^3}\int_\beta^1\int_\alpha^1 \xi^{3r}\eta^{3s}\left\{\left(\frac{\partial\Psi_\xi}{\partial\xi}+\left(\frac{A}{B}\right)^2\frac{\partial\Psi_\eta}{\partial\eta}\right)^2 - 2(1-\nu)\left(\frac{A}{B}\right)^2\left[\frac{\partial\Psi_\xi}{\partial\xi}\frac{\partial\Psi_\eta}{\partial\eta}\right.\right.$$
$$\left.\left. -\frac{1}{4}\left(\frac{\partial\Psi_\xi}{\partial\eta}+\frac{\partial\Psi_\eta}{\partial\xi}\right)^2\right] + \frac{\kappa G h_0}{D_0}A^2\xi^r\eta^s\left[\left(\Psi_\xi+\frac{\partial W}{\partial\xi}\right)^2+\left(\frac{A}{B}\right)^2\left(\Psi_\eta+\frac{\partial W}{\partial\eta}\right)^2\right]\right\}\mathrm{d}\xi\mathrm{d}\eta, \tag{3}$$
$$T_{max} = \frac{1}{2}\rho h_0\omega^2 AB\int_\beta^1\int_\alpha^1 \xi^r\eta^s\left[W^2+\frac{1}{12}\left(\frac{h_0}{B}\right)^2\xi^{2r}\eta^{2s}(\Psi_\xi^2/\lambda^2+\Psi_\eta^2)\right]\mathrm{d}\xi\,\mathrm{d}\eta$$

in which, $W(\xi,\eta)$ is the dynamic displacement function of the plate, $\Psi_\xi(\xi,\eta)$ and $\Psi_\eta(\xi,\eta)$ are, respectively, the dynamic rotation-angle functions due to bending in the ξ and η directions, ω is the radian eigenfrequency of the plate, $D_0 = Eh_0^3/[12(1-\nu^2)]$ is the flexural rigidity of the plate at the point $\xi=1$, $\eta=1$, $G = E/[2(1+\nu)]$ is the elastic modulus of shear, κ is the shear correction factor, ν is the Poisson ratio, E is Young's modulus and ρ is the density of the plate per unit volume.

Assuming that $W(\xi,\eta)$, $\Psi_\xi(\xi,\eta)$ and $\Psi_\eta(\xi,\eta)$ are all separable functions in variations and can be written in the form of

$$W(\xi,\eta) = \sum_{i=i_0}^{\infty}\sum_{j=j_0}^{\infty} c_{ij}X_i(\xi)Y_j(\eta), \qquad \Psi_\xi(\xi,\eta) = \sum_{i=i_0}^{\infty}\sum_{j=j_0}^{\infty} d_{ij}\Phi_i(\xi)Y_j(\eta)/A,$$
$$\Psi_\eta(\xi,\eta) = \sum_{i=i_0}^{\infty}\sum_{j=j_0}^{\infty} e_{ij}X_i(\xi)\Psi_j(\eta)/B, \tag{4}$$

where c_{ij}, d_{ij} and e_{ij} are the unknown constants, $X_i(\xi)$, $\Phi_i(\xi)$ and $Y_j(\eta)$, $\Psi_j(\eta)$ are the appropriate admissible functions, respectively, in the ξ and η directions. i_0 and j_0 are the beginning order of the admissible functions in the ξ and η directions, respectively. For plates truncated in both directions, $i_0 = j_0 = 0$, however, for plates with sharp ends, i_0 and/or j_0 should be decided by the taper factors, which will be discussed later.

Truncating the series variations i and j in Eq. (4) up to i_0+I and j_0+J, respectively, then applying the Rayleigh–Ritz method

$$\frac{\partial \Pi}{\partial c_{ij}}=0, \qquad \frac{\partial \Pi}{\partial d_{ij}}=0, \qquad \frac{\partial \Pi}{\partial e_{ij}}=0, \tag{5}$$
$$i=i_0,i_0+1,i_0+2,\ldots,i_0+I, \quad j=j_0,j_0+1,j_0+2,\ldots,j_0+J$$

one has the eigenfrequency equation as follows:

$$\left([K]-\frac{\Omega^2}{(1-\alpha)^4}[M]\right)\begin{Bmatrix}\{c\}\\ \{d\}\\ \{e\}\end{Bmatrix}=\{0\} \tag{6}$$

in which, $\Omega^2=\omega^2\rho h_0 a^4/D_0$ is the non-dimensional eigenfrequency, $\lambda=a/b$ is the aspect ratio of the plate. $[K]$ is the stiffness matrix of the plate, $[M]$ is the mass matrix of the plate, $\{c\}$, $\{d\}$ and $\{e\}$ are the column matrices of the unknown constants, which are, respectively, given as follows:

$$\begin{aligned}
\{c\}&=[c_{i_0j_0},c_{i_0j_0+1},\ldots,c_{i_0j_0+J},c_{i_0+1j_0},c_{i_0+1j_0+1},\ldots,c_{i_0+1j_0+J},\ldots,c_{i_0+Ij_0},c_{i_0+Ij_0+1},\ldots,c_{i_0+Ij_0+J}]^{\mathrm{T}},\\
\{d\}&=[d_{i_0j_0},d_{i_0j_0+1},\ldots,d_{i_0j_0+J},d_{i_0+1j_0},d_{i_0+1j_0+1},\ldots,d_{i_0+1j_0+J},\ldots,d_{i_0+Ij_0},d_{i_0+Ij_0+1},\ldots,d_{i_0+Ij_0+J}]^{\mathrm{T}},\\
\{e\}&=[e_{i_0j_0},e_{i_0j_0+1},\ldots,e_{i_0j_0+J},e_{i_0+1j_0},e_{i_0+1j_0+1},\ldots,e_{i_0+1j_0+J},\ldots,e_{i_0+Ij_0},e_{i_0+Ij_0+1},\ldots,e_{i_0+Ij_0+J}]^{\mathrm{T}}
\end{aligned} \tag{7}$$

and

$$[K]=\begin{bmatrix}[K_{cc}] & [K_{cd}] & [K_{ce}]\\ & [K_{dd}] & [K_{de}]\\ \textit{symmetric} & & [K_{ee}]\end{bmatrix}, \qquad [M]=\begin{bmatrix}[M_{cc}] & [M_{cd}] & [M_{ce}]\\ & [M_{dd}] & [M_{de}]\\ \textit{symmetric} & & [M_{ee}]\end{bmatrix}, \tag{8}$$

where

$$\begin{aligned}
K_{ccimjn}&=(E^{1,1}_{im}F^{0,0}_{jn}+\Gamma^2E^{0,0}_{im}F^{1,1}_{jn})/R, \qquad K_{cdimjn}=T^{1,0}_{im}F^{0,0}_{jn}/R,\\
K_{ceimjn}&=\Gamma^2E^{0,0}_{im}U^{1,0}_{jn}/R, \qquad K_{ddimjn}=\bar{G}^{1,1}_{im}\bar{F}^{0,0}_{jn}+(1-v)\Gamma^2\bar{G}^{0,0}_{im}\bar{F}^{1,1}_{jn}/2+G^{0,0}_{im}F^{0,0}_{jn}/R,\\
K_{deimjn}&=\lambda^2[v\bar{O}^{1,0}_{im}\bar{U}^{0,1}_{jn}+(1-v)\bar{O}^{0,1}_{im}\bar{U}^{1,0}_{jn}/2],\\
K_{eeimjn}&=\Gamma^4\bar{E}^{0,0}_{im}\bar{H}^{1,1}_{jn}+(1-v)\Gamma^2\bar{E}^{1,1}_{im}\bar{H}^{0,0}_{jn}/2+\Gamma^2E^{0,0}_{im}H^{0,0}_{jn}/R,\\
M_{ccimjn}&=E^{0,0}_{im}F^{0,0}_{jn}, \qquad M_{ddimjn}=\gamma^2\bar{G}^{0,0}_{im}\bar{F}^{0,0}_{jn}/(12\Gamma^2),\\
M_{eeimjn}&=\gamma^2\bar{E}^{0,0}_{im}\bar{H}^{0,0}_{jn}/12, \qquad M_{cdimjn}=M_{ceimjn}=M_{deimjn}=M_{eeimjn}=0
\end{aligned} \tag{9}$$

in which,

$$E_{im}^{p,q}=\int_{\alpha}^{1}\xi^{r}\frac{\mathrm{d}^{p}X_{i}(\xi)}{\mathrm{d}\xi^{r}}\frac{\mathrm{d}^{q}X_{m}(\xi)}{\mathrm{d}\xi^{s}}\mathrm{d}\xi,\qquad G_{im}^{p,q}=\int_{\alpha}^{1}\xi^{r}\frac{\mathrm{d}^{p}\Phi_{i}(\xi)}{\mathrm{d}\xi^{r}}\frac{\mathrm{d}^{q}\Phi_{m}(\xi)}{\mathrm{d}\xi^{s}}\mathrm{d}\xi,$$

$$T_{im}^{p,q}=\int_{\alpha}^{1}\xi^{r}\frac{\mathrm{d}^{p}X_{i}(\xi)}{\mathrm{d}\xi^{r}}\frac{\mathrm{d}^{q}\Phi_{m}(\xi)}{\mathrm{d}\xi^{s}}\mathrm{d}\xi,\qquad F_{jn}^{p,q}=\int_{\beta}^{1}\eta^{s}\frac{\mathrm{d}^{p}Y_{j}(\eta)}{\mathrm{d}\eta^{r}}\frac{\mathrm{d}^{q}Y_{n}(\eta)}{\mathrm{d}\eta^{s}}\mathrm{d}\eta,$$

$$H_{jn}^{p,q}=\int_{\beta}^{1}\eta^{s}\frac{\mathrm{d}^{p}\Psi_{j}(\eta)}{\mathrm{d}\eta^{r}}\frac{\mathrm{d}^{q}\Psi_{n}(\eta)}{d\eta^{s}}\mathrm{d}\eta,\qquad U_{jn}^{p,q}=\int_{\beta}^{1}\eta^{s}\frac{\mathrm{d}^{p}Y_{j}(\eta)}{\mathrm{d}\eta^{r}}\frac{\mathrm{d}^{q}\Psi_{n}(\eta)}{\mathrm{d}\eta^{s}}\mathrm{d}\eta,$$

$$\bar{O}_{im}^{p,q}=\int_{\alpha}^{1}\xi^{3r}\frac{\mathrm{d}^{p}\Phi_{i}(\xi)}{\mathrm{d}\xi^{r}}\frac{\mathrm{d}^{q}X_{m}(\xi)}{\mathrm{d}\xi^{s}}\mathrm{d}\xi,\qquad \bar{G}_{im}^{p,q}=\int_{\alpha}^{1}\xi^{3r}\frac{\mathrm{d}^{p}\Phi_{i}(\xi)}{\mathrm{d}\xi^{r}}\frac{\mathrm{d}^{q}\Phi_{m}(\xi)}{\mathrm{d}\xi^{s}}\mathrm{d}\xi,$$

$$\bar{E}_{im}^{p,q}=\int_{\alpha}^{1}\xi^{3r}\frac{\mathrm{d}^{p}X_{i}(\xi)}{\mathrm{d}\xi^{r}}\frac{\mathrm{d}^{q}X_{m}(\xi)}{\mathrm{d}\xi^{s}}\mathrm{d}\xi,\qquad \bar{U}_{jn}^{p,q}=\int_{\beta}^{1}\eta^{3s}\frac{\mathrm{d}^{p}Y_{j}(\eta)}{\mathrm{d}\eta^{r}}\frac{\mathrm{d}^{q}\Psi_{n}(\eta)}{\mathrm{d}\eta^{s}}\mathrm{d}\eta,$$

$$\bar{F}_{jn}^{p,q}=\int_{\beta}^{1}\eta^{3s}\frac{\mathrm{d}^{p}Y_{j}(\eta)}{\mathrm{d}\eta^{r}}\frac{\mathrm{d}^{q}Y_{n}(\eta)}{\mathrm{d}\eta^{s}}\mathrm{d}\eta,\qquad \bar{H}_{jn}^{p,q}=\int_{\beta}^{1}\eta^{3s}\frac{\mathrm{d}^{p}\Psi_{j}(\eta)}{\mathrm{d}\eta^{r}}\frac{\mathrm{d}^{q}\Psi_{n}(\eta)}{\mathrm{d}\eta^{s}}\mathrm{d}\eta,$$

$$p,q=0,1,\quad i,m=1,2,3,\ldots,I,\quad j,n=1,2,3,\ldots,J,$$

$$\Gamma^{2}=\lambda^{2}(1-\beta)^{2}/(1-\alpha)^{2},\qquad \lambda=a/b,\qquad \gamma=h_{0}/b,\qquad R=\frac{D_{0}}{\kappa G h_{0}b^{2}\lambda^{2}}. \tag{10}$$

Here R is referred to as the shear correction coefficient of Mindlin plates.

Integrals in Eq. (10) can be numerically evaluated by the piecewise Gaussian quadrature. Resolving Eq. (6) by the standard eigenvalue program, the dimensionless eigenfrequencies Ω and the coefficients $\{c\}$, $\{d\}$ and $\{e\}$ can be easily obtained. Substituting the results into Eq. (4) gives the corresponding mode shapes.

3. Two sets of static Timoshenko beam functions (STBF)

A unit width strip taken from the tapered rectangular plate in one or the other direction, as shown in Fig. 1(b1)-(b3), is used to derive the admissible functions of the plate. Without loss of generality, only the strip in the x direction is considered because the tapered plates investigated here are with similar thickness variation in both directions. The differential characteristic equation of the tapered Timoshenko beam under a transverse non-dimensional static load $Q(\xi)$ can be given as follows:

$$\delta\frac{\mathrm{d}}{\mathrm{d}\xi}\left\{\xi^{r}\left[\frac{\mathrm{d}X(\xi)}{\mathrm{d}\xi}-\Phi(\xi)\right]\right\}=Q(\xi),$$

$$\frac{\mathrm{d}}{\mathrm{d}\xi}\left[\xi^{3r}\frac{\mathrm{d}\psi(\xi)}{\mathrm{d}\xi}\right]+\delta\xi^{r}\left[\frac{\mathrm{d}X(\xi)}{\mathrm{d}\xi}-\Phi(\xi)\right]=0, \tag{11}$$

where $X(\xi)$ is the flexural displacement and $\Phi(\xi)$ is the angle of rotation due to bending of the beam, $\delta=(1+\nu)(1-\alpha)^{2}h_{0}^{2}/(6\kappa a^{2})$. The bending moment $M(\xi)$ and the transverse shear force

$V(\xi)$ of the beam are, respectively, given as

$$M(\xi) = -\frac{Eh_0^3}{12a^2}(1-\alpha)^2\xi^{3r}\frac{\mathrm{d}\Phi(\xi)}{\mathrm{d}\xi}, \qquad V(\xi) = \frac{\kappa G h_0}{a}(1-\alpha)\xi^r\left[\frac{\mathrm{d}X(\xi)}{\mathrm{d}\xi} - \Phi(\xi)\right]. \tag{12}$$

At each end of the beam, two boundary equations can be established. Taking the end $\xi = \alpha$ as an example, one has

$$\begin{aligned} &Y(\alpha) = 0, \quad \psi(\alpha) = 0 \quad \text{for the clamped end,}\\ &Y(\alpha) = 0, \quad M(\alpha) = 0 \quad \text{for the simply supported end,}\\ &M(\alpha) = 0, \quad V(\alpha) = 0 \quad \text{for the free end.} \end{aligned} \tag{13}$$

Similarly, the boundary equations at the end $\xi = 1$ can also be given.

For an arbitrary load $Q(\xi)$, it can be expanded into a Taylor series as follows:

$$Q(\xi) = \sum_{i=0}^{\infty} Q_i(\xi - \xi_c)^i = \sum_{i=0}^{\infty} Q_i \sum_{k=0}^{i}(-1)^{i-k} D_k^i \xi_c^{i-k}\xi^k, \tag{14}$$

where ξ_c is the expanding point of the Taylor series and $D_k^i = i!/k!/(i-k)!$

The general solutions of the displacement and the angle of rotation due to bending can be obtained in the form of

$$X(\xi) = \sum_{i=0}^{\infty} Q_i X_i(\xi), \qquad \Phi(\xi) = \sum_{i=0}^{\infty} Q_i \Phi_i(\xi), \tag{15}$$

where

$$\begin{aligned} X_i(\xi) = &\sum_{k=0}^{i}(-1)^{i-k} D_k^i \xi_c^{i-k}[F^{1k}(\xi) - \delta F^{2k}(\xi)]\\ &+ [F_{01}(\xi) - \delta F_{02}(\xi)]C_0^i + F_1(\xi)C_1^i + \xi C_2^i + C_3^i, \end{aligned}$$

$$\Phi_i(\xi) = \sum_{k=0}^{i}(-1)^{i-k} D_k^i \xi_c^{i-k} f^k(\xi) + f_0(\xi)C_0^i + f_1(\xi)C_1^i + C_2^i \tag{16}$$

in which,

$$F^{1k}(\xi) = \frac{1}{(k+1)(k+2)}\begin{cases} \xi[\ln(\xi) - 1], & k = 3r-3,\\ \ln(\xi), & k = 3r-4,\\ \xi^{k+4-r}/[(k+3-3r)(k+4-3r)], & k \neq 3r-3, k \neq 3r-4 \end{cases}$$

$$F^{2k}(\xi)=\frac{1}{k+1}\begin{cases}\ln(\xi), & k=r-2,\\ \xi^{k+2-r}/(k+2-r), & k\neq r-2,\end{cases}$$

$$F_{01}(\xi)=\begin{cases}\xi[\ln(\xi)-1], & 3r=2,\\ \ln(\xi), & 3r=3,\\ \xi^{3-3r}/[(2-3r)(3-3r)], & 3r\neq 2, 3r\neq 3,\end{cases}$$

$$F_{02}(\xi)=\begin{cases}\ln(\xi), & r=1,\\ \xi^{1-r}/(1-r), & r\neq 1,\end{cases}$$

$$F_1(\xi)=\begin{cases}\xi[\ln(\xi)-1], & 3r=1,\\ \ln(\xi), & 3r=2,\\ \xi^{2-3r}/[(1-3r)(2-3r)], & 3r\neq 1, 3r\neq 2,\end{cases}$$

$$f^k(\xi)=\frac{1}{(k+1)(k+2)}\begin{cases}\ln(\xi), & k=3r-3,\\ \xi^{k+3-3r}/(k+3-3r), & k\neq 3r-3,\end{cases}$$

$$f_0(\xi)=\begin{cases}\ln(\xi), & 3r=2,\\ \xi^{2-3r}/(2-3r), & 3r\neq 2,\end{cases}$$

$$f_1(\xi)=\begin{cases}\ln(\xi), & 3r=1,\\ \xi^{1-3r}/(1-3r), & 3r\neq 1.\end{cases} \tag{17}$$

3.1. Truncated beam

For the truncated beams without rigid body movements, the unknown coefficients C_k^i $(k=1,2,3,4)$ in Eq. (16) can be uniquely decided by the four boundary equations of the beam for every i term. However, for a beam with rigid body movements, the coefficients in Eq. (16) cannot be determined directly from the boundary equations. In such a case, the static Timoshenko beam functions for the simply–simply supported beam can be used as the basis solutions supplemented by the modes of rigid body movements, which are described as follows:

BC	The first STBF	The second STBF	The third and higher STBF
F–F	$X_1(\xi)=1;$ $\Phi_1(\xi)=0$	$X_2(\xi)=\xi-(1-\alpha)/2;$ $\Phi_2(\xi)=1$	The first and higher STBF for the S–S beam
S–F	$X_1(\xi)=\xi-\alpha;$ $\Phi_1(\xi)=1$	The first STBF for the S–S beam	The second and higher STBF for the S–S beam
F–S	$X_1(\xi)=\xi-1;$ $\Phi_1(\xi)=1$	The first STBF for the S–S beam	The second and higher STBF for the S–S beam

3.2. Sharp-ended beam

For a sharp-ended beam, the sharp end cannot sustain a bending or a shear force, hence one has

$$C_0^i = 0, \qquad C_1^i = 0. \tag{18}$$

Moreover, the displacement and rotational angle of the beam should be finite at the sharp end, so that there is a limit to the order of the Taylor series load as follows:

$$i > 3r - 2. \tag{19}$$

Therefore, the beginning order of the Taylor series should be taken as

$$i_0 = \mathrm{Max}\{Int(3r - 1), 0\} \tag{20}$$

and Eq. (12) should be replaced by

$$Q(\xi) = \sum_{i=i_0}^{\infty} Q_i(\xi - \xi_c)^i = \sum_{i=i_0}^{\infty} Q_i \sum_{k=i_0}^{i} (-1)^{i-k} D_k^i \xi_c^{i-k} \xi^k. \tag{21}$$

For a cantilevered sharp-ended beam (F–C beam), the unknown coefficients C_2^i and C_3^i in Eq. (16) can be uniquely decided by the boundary equations of the beam at $\xi = 1$ for every i term. However, for a beam with rigid body movements, the static Timoshenko beam functions for the cantilevered sharp-ended beam should be used as the basis solutions supplemented by the modes of rigid body movements, which are described as follows:

BC	The first STBF	The second STBF	The third and higher STBF
F–F	$X_1(\xi) = 1;$ $\Phi_1(\xi) = 0$	$X_2(\xi) = \xi - 1;$ $\Phi_2(\xi) = 1$	The first and higher STBF for the F–C beam
F–S	$X_1(\xi) = \xi - 1;$ $\Phi_1(\xi) = 1$	The first STBF for the F–C beam	The second and higher STBF for the F–C beam

Now, we have obtained two sets of static Timoshenko beam functions as shown in Eq. (15), which can be used as the admissible functions of the plate in the x direction. Similarly, the admissible functions of the plate in the y direction can also be easily developed.

4. Convergence and comparison studies

Convergence and comparison studies have been carried out using the static Timoshenko beam functions derived in the last section as the admissible functions of the tapered rectangular Mindlin plates. It should be pointed out that when the midpoint of the beam is taken as the expanding point of the Taylor series, the best convergence is achieved. This phenomenon can be clearly explained: in the interval $[\alpha, 1]$, $\xi_c = (1 + \alpha)/2$ will result in the least convergence radius needed by the Taylor series expansion [21]. In all the following computations, $\xi_c = (1 + \alpha)/2$, shear correction factor $\kappa = \pi^2/12$ and the Poisson ratio $\nu = 0.3$ are used. Moreover, in order to increase the number of significant figures, quadruple precision is adopted in the computations. For the

sake of brevity, four capital letters are used to represent the boundary conditions of plates. The first two represent the boundary conditions of plates in the x direction and the other two represent those in the y direction. The first eight eigenfrequencies of simply supported and fully clamped square Mindlin plates with linearly varying thickness in the x direction and the thickness ratio $h_0/b = 0.3$ are given in Table 2 with respect to the number of terms of the admissible functions from 1×1 to 7×7 for two different truncation factors $\alpha = 0.25$ and 0.5. It can be seen that the convergent rate is quite rapid and in general, 5–7 terms of the static Timoshenko beam functions in each direction can give sufficiently satisfactory results for the first few eigenfrequencies. The comparison of the first seven eigenfrequencies for square Mindlin plates simply supported in the y direction and tapered in the x direction is given in Table 3 for two different thickness ratios $h_0/b = 0.2$ and 0.4 when the truncation factor $\beta = 0.5$. The reference data come from spline strip

Table 2
The convergence study on the first eight eigenfrequencies of square Mindlin plates with linearly varying thickness in one direction, $a/b = 1$, $r = 1$, $s = 0$ and $h_0/b = 0.3$

$I \times J$	Ω_1	Ω_2	Ω_3	Ω_4	Ω_5	Ω_6	Ω_7	Ω
$SS-SS$, $\alpha = 0.25$								
2×2	11.060	25.112	58.602	60.658	90.233	96.806	118.55	137.06
3×3	10.552	23.455	23.832	35.531	41.971	53.373	68.024	70.486
4×4	10.542	22.778	23.162	34.025	41.655	42.984	51.849	52.130
5×5	10.542	22.774	23.141	34.006	38.552	40.334	48.901	49.330
6×6	10.541	22.769	23.129	33.992	38.551	40.091	48.820	49.327
7×7	10.541	22.769	23.128	33.990	38.470	39.961	48.701	49.254
$CC-CC$, $\alpha = 0.25$								
2×2	16.716	31.740	40.595	48.820	114.99	120.17	126.65	128.89
3×3	16.108	29.874	31.544	41.599	50.015	58.471	77.291	81.815
4×4	16.053	28.495	28.881	39.044	48.146	49.809	56.258	57.353
5×5	16.041	28.437	28.873	39.022	43.881	44.885	53.125	53.194
6×6	16.041	28.400	28.588	38.841	43.855	44.580	52.851	53.188
7×7	16.040	28.398	28.587	38.838	43.660	44.360	52.681	53.057
$SS-SS$, $\alpha = 0.5$								
2×2	12.749	27.842	59.630	63.179	84.975	91.999	104.55	121.61
3×3	12.564	27.319	27.322	39.301	47.752	57.287	64.552	68.325
4×4	12.563	26.778	26.972	38.479	47.648	47.733	56.555	56.868
5×5	12.562	26.777	26.865	38.443	44.843	45.637	54.344	54.510
6×6	12.562	26.773	26.857	38.431	44.843	45.171	54.236	54.336
7×7	12.562	26.773	26.857	38.431	44.768	45.080	54.147	54.271
$CC-CC$, $\alpha = 0.5$								
2×2	18.853	33.574	39.871	48.779	102.59	107.82	115.89	118.84
3×3	18.575	32.713	33.503	44.201	52.868	61.179	73.696	79.059
4×4	18.549	31.978	32.017	42.743	51.745	53.011	60.035	60.690
5×5	18.536	31.857	32.008	42.703	48.531	49.494	57.377	57.768
6×6	18.536	31.830	31.930	42.624	48.368	49.053	57.323	57.359
7×7	18.535	31.828	31.930	42.624	48.235	48.906	57.206	57.254

Table 3
The comparison of eigenfrequencies of square Mindlin plates simply supported in one direction and with linearly varying thickness in the other direction, $r = 1$, $s = 0$, $\beta = 0.5$

h_0/b	Ω_1/β	Ω_2/β	Ω_3/β	Ω_4/β	Ω_5/β	Ω_6/β	Ω_7/β
SS−SS							
0.2	27.118	61.382	61.737	92.011	108.34	109.88	135.09
Mizusawa [15]	27.118	61.382	61.737	92.011	108.33	109.86	135.09
Mikami et al. [13]	27.11	60.56	61.73	92.02	108.3	109.9	135.1
Aksu et al. [14]	26.175	60.674	60.965	88.808	108.29		
0.4	23.025	46.590	46.658	64.834	74.896	75.116	88.916
Mizusawa [15]	23.025	46.590	46.658	64.834	74.895	75.108	88.912
Mikami et al. [13]	23.02	46.59	46.65	64.83	74.89		
Aksu et al. [14]	21.595	45.061	45.182	61.781	71.716		
SS − CC							
0.2	36.063	65.232	75.692	100.16	110.52	123.91	139.96
Mizusawa [15]	36.063	65.231	75.690	100.15	110.52	123.87	139.96
Mikami et al. [13]	36.07	65.23	75.68	100.2	110.5		
Aksu et al. [14]	36.524	65.490	77.879	99.699	111.32		
0.4	27.353	47.830	50.892	66.818	75.368	77.764	89.894
Mizusawa [15]	27.353	47.830	50.892	66.818	75.367	77.754	89.893
Mikami et al. [13]	27.35	47.82	50.90	66.82	75.37		
Aksu et al. [14]	27.240	47.290	50.245	64.856	73.029		
SS−FF							
0.2	13.840	22.562	46.757	46.979	61.386	82.738	87.506
Mizusawa [15]	13.816	22.530	46.709	46.939	61.291	82.696	87.517
Mikami et al. [13]	13.82	22.52	46.71	46.93	61.30		
0.4	12.586	19.095	36.586	37.800	45.276	58.736	61.113
Mizusawa [15]	12.569	19.084	36.584	37.769	45.247	58.727	61.106
Mikami et al.[13]	12.57	19.08	36.58	37.77	45.25		
SS−SF							
0.2	17.660	36.091	56.783	72.260	73.247	104.90	106.86
Mizusawa [15]	17.626	36.066	56.718	72.163	73.224	104.82	106.83
0.4	15.379	28.785	42.721	52.216	52.742	70.756	72.961
Mizusawa [15]	15.360	28.784	42.695	52.209	52.742	70.751	72.944

Table 3

method [15], collocation method [13] and variational method in conjunction with the finite difference technique [14], respectively. It is found that very good agreement has been obtained for all cases.

The comparison study on the first three eigenfrequencies for simply–simply supported square Mindlin plates tapered in one or two directions and with a thickness ratio $h_0/b = 0.4$ is given in Table 4 by using the vibrating Timoshenko beam functions and the static Timoshenko beam functions, respectively. Three kinds of taper factors (linearly varying thickness in one direction: $r = 1$, $s = 0$; linearly varying thickness in both directions: $r = 1$, $s = 1$; parabolically varying thickness in one direction: $r = 2$, $s = 0$) and three different truncation factors ($\alpha = \beta = 0.1$, $0.3, 0.5$) are considered. It can be seen that for plates with small truncation factors, the results of

Table 4
The comparison of first three eigenfrequencies of simply supported square Mindlin plates tapered in one or two directions and with a thickness ratio $h_0/b = 0.4$ by using the STBF and the vibrating Timoshenko beam functions (VTBF), respectively

r, s	Method	$I \times J$	Ω_1	Ω_2	Ω_3
$\alpha = \beta = 0.1$					
1,0	STBF	5×5	8.4812	17.583	18.058
	VTBF	5×5	8.6657	18.083	18.769
		8×8	8.5417	17.771	18.287
1,1	STBF	5×5	4.6896	8.6528	10.556
	VTBF	5×5	4.9265	9.5896	11.355
		8×8	4.7612	8.8453	10.795
2,0	STBF	5×5	5.3347	8.1223	9.7717
	VTBF	5×5	6.1730	10.820	13.015
		8×8	5.7325	9.3740	11.194
$\alpha = \beta = 0.3$					
1,0	STBF	5×5	10.236	21.175	21.320
	VTBF	5×5	10.266	21.269	21.423
		8×8	10.254	21.246	21.374
1,1	STBF	5×5	7.0942	14.944	15.925
	VTBF	5×5	7.1237	15.065	16.026
		8×8	7.1055	14.978	15.960
2,0	STBF	5×5	7.3204	14.525	15.457
	VTBF	5×5	7.4570	14.984	16.093
		8×8	7.3543	14.654	15.576
$\alpha = \beta = 0.5$					
1,0	STBF	5×5	11.512	23.300	23.336
	VTBF	5×5	11.537	23.377	23.407
		8×8	11.535	23.374	23.402
1,1	STBF	5×5	9.3077	19.654	19.990
	VTBF	5×5	9.3254	19.704	20.043
		8×8	9.3223	19.696	20.035
2,0	STBF	5×5	9.3800	19.498	19.792
	VTBF	5×5	9.4056	19.592	19.898
		8×8	9.3940	19.565	19.840

vibrating Timoshenko beam functions are obviously lower in accuracy and slower in convergence than those of static Timoshenko beam functions developed in this paper because of the Rayleigh–Ritz method invariably gives the upper bound values of the exact eigenfrequencies. This is always true for a rectangular Mindlin plate with any taper factor and truncation factor although the vibrating Timoshenko beam functions used here are exact solutions for a uniform Mindlin plate with four simply supported edges.

5. Numerical results

A survey on the literature quickly reveals that the study on vibrations of tapered rectangular Mindlin plates are very limited and the only results available are for Mindlin plates with two

opposite edges simply supported and tapered in one direction. In this section, some first-time reported results are given. In Table 5, the first seven eigenfrequencies of sharp-ended rectangular Mindlin plates with linearly varying thickness in the x direction are given for various thickness ratios from 0.05 to 0.4. Two kinds of boundary conditions (cantilevered plates: FC–FF and fully free plates: FF–FF) and three different aspect ratios ($a/b = 0.5, 1, 2$) are considered. It can be seen that the effect of the thickness ratio on eigenfrequencies decreases with the increase of the aspect ratio of the plates. In Figs. 2 and 3, the first two eigenfrequencies of a square Mindlin plate with linearly varying thickness in two directions are given. The truncation factors of the plate are the same in both directions: $\alpha = \beta = 0.5$. Six kinds of boundary conditions are considered. From the

Table 5
The first seven eigenfrequencies of sharp-ended rectangular Mindlin Plates with linearly varying thickness in one direction, $r = 1$, $s = 0$

a/b	h_0/b	Ω_1	Ω_2	Ω_3	Ω_4	Ω_5	Ω_6	Ω_7
FC−FF								
0.5	0.05	5.2449	5.7259	7.2308	9.5900	12.455	14.905	15.238
	0.1	5.1383	5.6041	7.0688	9.3703	12.174	14.262	14.568
	0.2	4.7815	5.2092	6.5533	8.6798	11.276	12.368	12.605
	0.3	4.3257	4.7183	5.9286	7.8499	10.081	10.537	10.654
	0.4	3.8614	4.2244	5.3121	7.0276	8.7187	9.0807	9.2198
1.0	0.05	5.2328	7.2257	12.171	15.029	16.610	18.731	22.835
	0.1	5.1986	7.1747	12.065	14.847	16.350	18.599	22.433
	0.2	5.0864	7.0053	11.740	14.207	15.546	18.160	21.231
	0.3	4.9257	6.7621	11.301	13.324	14.502	17.543	19.742
	0.4	4.7298	6.4674	10.778	12.346	13.379	16.802	18.190
2.0	0.05	5.1788	11.477	14.869	21.485	24.035	29.595	36.128
	0.1	5.1634	11.420	14.810	21.314	23.968	29.420	35.889
	0.2	5.1252	11.255	14.613	20.823	23.759	28.807	35.031
	0.3	5.0752	11.049	14.328	20.201	23.479	27.904	33.746
	0.4	5.0142	10.803	13.966	19.480	23.130	26.799	32.191
FF−FF[a]								
0.5	0.05	3.6045	4.7768	8.4662	8.4773	12.224	12.708	13.028
	0.1	3.5591	4.5347	8.2042	8.2697	11.914	12.407	12.520
	0.2	3.3995	4.0009	7.4586	7.6193	10.906	11.090	11.458
	0.3	3.1854	3.4547	6.5945	6.8187	9.6017	9.6672	10.311
	0.4	2.9455	2.9546	5.7395	6.0025	8.2731	8.4256	9.0000
1.0	0.05	8.1808	11.169	12.777	17.422	17.490	18.829	24.830
	0.1	8.0863	11.073	12.692	17.137	17.206	18.664	24.618
	0.2	7.8420	10.764	12.379	16.244	16.444	18.193	23.846
	0.3	7.5292	10.338	11.920	15.185	15.420	17.563	22.529
	0.4	7.1690	9.8338	11.367	14.072	14.319	16.815	20.846
2.0	0.05	12.343	13.180	24.047	25.037	27.225	37.893	41.683
	0.1	12.313	13.131	23.977	24.828	27.119	37.758	41.249
	0.2	12.211	12.999	23.761	24.303	26.739	37.327	40.113
	0.3	12.061	12.825	23.472	23.654	26.171	36.642	38.812
	0.4	11.868	12.610	22.905	23.113	25.458	35.570	37.622

[a] The zero eigenfrequencies are not included.

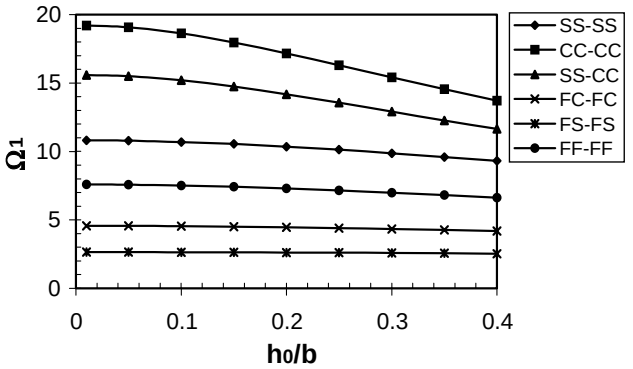

Fig. 2. The fundamental eigenfrequency of a square Mindlin plate with linearly varying thickness and the same truncation factors in two directions ($\alpha = \beta = 0.5$, $r = s = 1$).

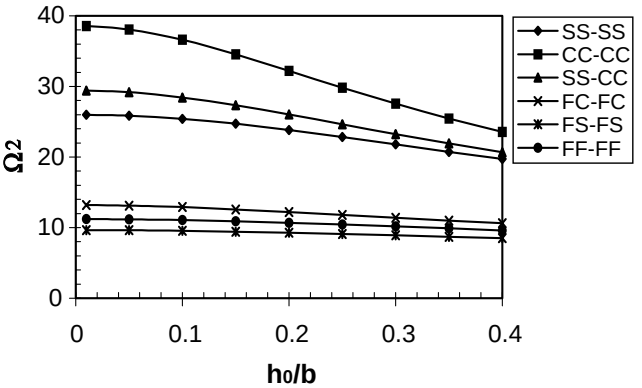

Fig. 3. The second order of eigenfrequency of a square Mindlin plate with linearly varying thickness and the same truncation factors in two directions ($\alpha = \beta = 0.5$, $r = s = 1$).

figures, one can find that the effect of thickness ratio on eigenfrequencies increases with the increase of boundary constraints of the plates. Thus, the thickness ratio of fully clamped plates has the biggest effect on eigenfrequencies and that of fully free plates has the least effect on eigenfrequencies (if zero eigenfrequencies are included). Moreover, it is shown that the eigenfrequencies monotonically decrease with increases in the thickness ratio and the effect of the thickness ratio on eigenfrequencies increases with increases in the frequency order. In Figs. 4 and 5, the first five eigenfrequencies of a cantilevered square Mindlin plate (FC–FF) with linearly varying thickness in the x direction are given with respect to two different thickness ratios $h_0/b = 0.1$ and 0.2, respectively. It is shown that the effect of the truncation factors on eigenfrequencies increases with increases in the frequency order. Furthermore, it is seen that the fundamental eigenfrequency decreases monotonically with the increase of the truncation factors, however the higher order eigenfrequencies increase with the increase of the truncation factors for the plates with truncation $\alpha \geqslant 0.2$. The different varying trends of the fundamental eigenfrequency and the

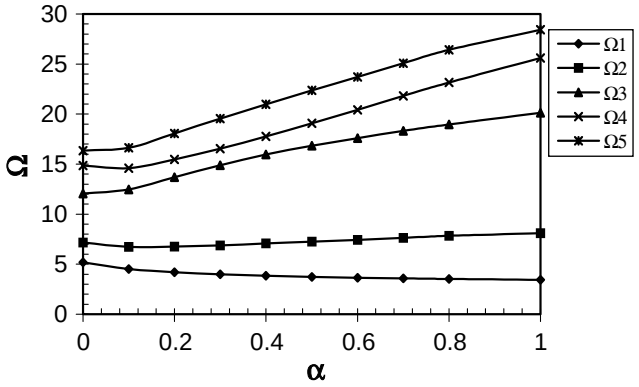

Fig. 4. The first five eigenfrequencies of a cantilevered square Mindlin plate with linearly varying thickness in one direction ($r = 1$; $s = 0$) for $h_0/b = 0.1$.

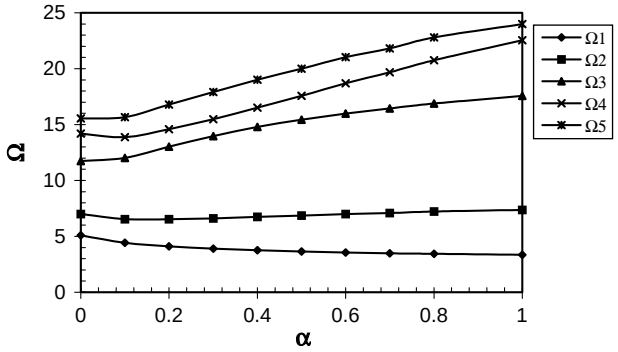

Fig. 5. The first five eigenfrequencies of a cantilevered square Mindlin plate with linearly varying thickness in one direction ($r = 1$; $s = 0$) for $h_0/b = 0.2$.

higher order eigenfrquencies with truncation factors can be explained as follows. As the truncation factors increase, both the stiffness and the mass of the plate increase. An increase in stiffness will result in an increase in the eigenfrequency, whereas an increase in mass will result in a decrease in the eigenfrequency. In most cases, however, the eigenfrequencies (especially for the higher order ones) increase as the truncation factors increase.

6. Concluding remarks

The free vibrations of rectangular Mindlin plates with variable thickness in one or two directions are investigated by using the Rayleigh–Ritz method. The variation of the thickness is described by a power function of the Cartesian co-ordinates. The static Timoshenko beam functions are developed from a unit width strip taken from the plate in some direction under a

Taylor series of static load as the admissible functions of the plate in that direction. Unlike conventional basis functions such as the vibrating Timoshenko beam functions for uniform Timoshenko beams, which are independent of the thickness variation of the plate, the static Timoshenko beam functions presented in this paper are closely connected with the thickness variation of the plate. Therefore, more rapid convergence and higher accuracy can be expected, especially for plates with small truncation factors. The comparison and convergence study shows that the first few eigenfrequencies can be given with sufficiently satisfactory accuracy by using only a small number of terms of the static Timoshenko beam functions. Finally, some valuable results are presented.

Acknowledgements

The financial support from a CRCG research grant of the University of Hong Kong is gratefully acknowledged.

References

[1] S.P. Timoshenko, S. Woinowsky-Krieger, Theory of Plates and Shells, McGraw-Hill, New York, 1959.
[2] R.D. Mindlin, Influence of rotary inertia and shear in flexural motion of isotropic, elastic plates, Transactions of the American Society of Mechanical Engineers, Journal of Applied Mechanics 18 (1951) 31–38.
[3] R.D. Mindlin, A. Schacknow, H. Deresiewicz, Flexural vibrations of rectangular plates, Transactions of the American Society of Mechanical Engineers, Journal of Applied Mechanics 23 (1956) 430–436.
[4] P.R. Benson, E. Hinton, A thick finite strip solution for static, free vibration and stability problem, International Journal for Numerical Methods in Engineering 10 (1976) 665–678.
[5] D.J. Dawe, Finite strip models for vibration of Mindlin plates, Journal of Sound and Vibration 59 (1978) 441–452.
[6] K.M. Liew, Y. Xiang, S. Kitipornchai, Transverse vibration of thick rectangular plates—I. Comprehensive sets of boundary conditions, Computers and Structures 49 (1993) 1–29.
[7] K.M. Liew, C.M. Wang, Y. Xiang, S. Kitipornchai, Vibration of Mindlin Plates, Elsevier, Oxford, 1998.
[8] K.M. Liew, K.C. Hung, M.K. Lim, A continuum three-dimensional vibration analysis of thick rectangular plates, International Journal of Solids and Structures 30 (1993) 3357–3379.
[9] C.C. Chen, K.M. Liew, C.W. Lim, S. Kitipornchai, Vibration analysis of symmetrically laminated thick rectangular plates using the higher-order theory, Journal of the Acoustical Society of America 102 (1997) 1600–1611.
[10] F.C. Appl, N.R. Byers, Fundamental frequency of simply supported rectangular plate with linearly varying thickness, Transactions of American Society of Mechanical Engineers, Journal of Applied Mechanics 32 (1965) 163–168.
[11] V.A. Pulmano, R.K. Gupta, Vibration of tapered plates by finite strip method, American Society of Civil Engineers, Journal of the Engineering Mechanics Division 102 (1976) 553–559.
[12] Y.K. Cheung, D. Zhou, The free vibrations of tapered rectangular plates using a new set of beam functions with the Rayleigh–Ritz method, Journal of Sound and Vibration 223 (1999) 703–722.
[13] T. Mikami, J. Yoshimura, Application of the collocation method to vibration analysis of rectangular Mindlin plates, Computers and Structures 18 (1984) 425–431.
[14] G. Aksu, S.A. Al-Kaabi, Free vibration analysis of Mindlin plates with linearly varying thickness, Journal of Sound and Vibration 119 (1987) 189–205.
[15] T. Mizusawa, Vibration of rectangular Mindlin plates with tapered thickness by the spline strip method, Computers and Structures 46 (1993) 451–463.

[16] S.A. Al-Kaabi, G. Aksu, Natural frequencies of Mindlin plates of bilinearly varying thickness, Journal of Sound and Vibration 123 (1988) 373–379.
[17] S.A. Al-Kaabi, G. Aksu, Free vibration analysis of Mindlin plates with parabolically varying thickness, Computers and Structures 34 (1990) 395–399.
[18] H. Mutsuda, T. Sakiyama, Discrete method of analyzing the bending vibration of skew Mindlin plates with variable thickness, Journal of Sound and Vibration 127 (1988) 179–186.
[19] K.M. Liew, Y. Xiang, S. Kitipornchai, Research on thick plate vibration: a literature survey, Journal of Sound and Vibration 180 (1995) 163–176.
[20] D. Zhou, Y.K. Cheung, Vibrations of tapered Timoshenko beams in terms of static beam functions, Transactions of American Society of Mechanical Engineers, Journal of Applied Mechanics 68 (2001) 596–602.
[21] D. Zhou, Y.K. Cheung, The free vibration of a type of tapered beams, Computer Methods in Applied Mechanics and Engineering 188 (2000) 203–216.